ISSN 0030-400X, Optics and Spectroscopy, 2017, Vol. 122, No. 2, pp. 207–213. © Pleiades Publishing, Ltd., 2017.
Original Russian Text © E.V. Seliverstova, N.Kh. Ibrayev, 2017, published in Optika i Spektroskopiya, 2017, Vol. 122, No. 2, pp. 228–235.

CONDENSED-MATTER SPECTROSCOPY

The Effect of Orientation and Distance between Donor and Acceptor Molecules on the Efficiency of Singlet–Singlet Energy Transfer in Langmuir–Blodgett Films

E. V. Seliverstova and N. Kh. Ibrayev*

Institute of Molecular Nanophotonics, Buketov Karaganda State University, Karaganda, 100028 Kazakhstan

**e-mail: niazibrayev@mail.ru*

Received July 5, 2016

Abstract—Singlet–singlet energy transfer between molecules of fluorescein and oxazine dyes in Langmuir–Blodgett films is studied experimentally. The dependence of the energy-transfer efficiency on the distance shows that the quenching of the donor fluorescence is the most efficient when the layers of the donor and acceptor molecules are in a direct contact. An increase in the distance between the donor and acceptor layers leads to a decrease in the energy-transfer efficiency. To establish the mutual orientation of the donor and acceptor molecules, quantum-chemical calculations of the energy transfer process in the donor–acceptor pair are carried out. The calculations show that the best correlation of the experimental and calculated values of the energy-transfer efficiency is observed when the interacting particles are shifted relative to each other by about ~0.12 nm in parallel planes. The presented approach can be used to estimate the relative orientation of interacting particles in multimolecular ensembles.

DOI: 10.1134/S0030400X17020242

INTRODUCTION

Intermolecular transfer of electronic excitation energy is one of the key processes in the transformation of absorbed light into energy of other types [1, 2]. Depending on the type of interaction between the particles, the energy transfer is due to either the exchange or the inductive-resonance mechanism [3, 4].

Currently, inductive-resonance energy transfer is the subject of active interest in connection with the prospects of its use in dye-sensitized photovoltaic solar cells [5, 6] and for studies of the formation and morphology of metal nanoparticles in solutions [7, 8].

In addition, this type of energy transfer is used to identify the localization and interaction of proteins, including proteins inside cells [9] and conformational changes in DNA [10].

Evaluation of the energy-transfer efficiency requires taking into account factors of distance and orientation [4, 11]. For experimental studies of their influence on the energy-transfer efficiency one can use the Langmuir–Blodgett (LB) method, which allows preparation of donor–acceptor systems with controlled distance between the reactants and their mutual orientation [12]. The use of this method provides the ability to control the efficiency of energy transfer from donor to acceptor in nanostructures.

Orientation factor k^2 depends on the relative orientation of the transition-dipole moments of the donor and the acceptor. The orientation of the chromophores can be estimated by measuring polarization in the absorption or fluorescence [13]. This method is well suited for determining the direction of the transition-moment vector in the case of linear molecules with their pronounced anisotropy of the electronic transition. Rigid chemical bonding of particles is another way to create donor–acceptor pairs with a fixed mutual orientation of the molecules [14, 15].

In addition to experimental methods [16], the efficiency of energy transfer can be evaluated with the use of a quantum-chemical method [17–19]. Computational chemistry in combination with experiment is widely used to study the distribution of particles in molecular clusters [20] and photophysical processes in nanosized systems [21]. The methods of molecular dynamics are widely used in studies of molecular and biological systems [22, 23].

In the present work, interlayer singlet–singlet energy transfer in nanoscale LB films is studied experimentally. The dependence of the energy-transfer efficiency on the distance between the donor and acceptor layers is obtained. Mutual orientation of the donor and acceptor molecules in the LB films is determined using values of the energy-transfer rate constant

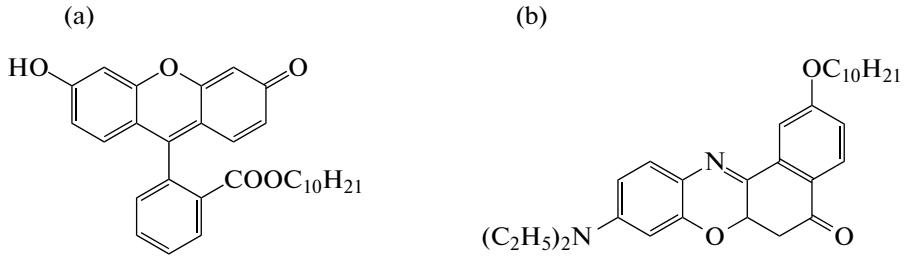

Fig. 1. The structural formula of (a) donor and (b) acceptor.

obtained from experimental data and from quantum-chemical modeling.

EXPERIMENT

Donor–acceptor structures were obtained with the use of the LB method on the basis of organic dyes and amphiphilic polyampholyte (PDAOM) [24]. The energy donor was decyl ether of fluorescein (DEF), and the acceptor was oxazine-41, an amphiphilic analogue of Nile red. Structural formulas of the used compounds are shown in Fig. 1.

Donor–acceptor systems were prepared using a Langmuir bath (KSV Nima Medium) in the following way. Dyes and polyampholyte were separately dissolved in chloroform and then mixed in the desired ratios. The concentration of donor molecules in the solution was constant and equal to 20 mol % relative to PDAOM. The concentration of the acceptor in the solution was varied from 5 to 20 mol %. The resulting solution was applied on the surface of the water–air interphase. Then the mixed monolayer of the donor with polyampholytes was transferred to the surface of glass substrates by the method of vertical lift of Y-type at surface pressure of $\pi = 25$ mN/m and speed of the substrate movement of 2 mm/min. The monolayer consisting of a mixture of the acceptor with PDAOM was applied on the top of the film prepared from the donor.

Deionized water purified by an AquaMax system was used as a subphase. The resistivity of the purified water was 18.2 MΩ/cm. The surface pressure was 72.8 mN/m at pH 5.6 and 20°C. The behavior of the monolayers on the water surface was studied by measuring the dependences of the surface pressure (π) on unit of the area (A) per molecule (π–A-isotherms). The surface pressure was measured with the use of a Wilhelmi balances. The rate of monolayer compression upon measuring of π–A isotherms or transferring the monolayer on a quartz glass substrate was 5 mm/min.

Fluorescence spectra of the prepared films were recorded on a Cary Eclipse spectrofluorimeter (Agilent). The lifetimes of the donor and acceptor fluorescence in the films were measured upon excitation at $\lambda_{ex} = 488$ nm with the use of a pulsed spectrofluorimeter with nanosecond resolution by the method of time-correlated photon counting (Becker&Hickl, Germany).

Theoretical calculations for the studied molecules were performed by the semiempirical quantum-chemical INDO method with a special spectroscopic parametrization [25], as well as by methods of molecular mechanics MM+. A theoretical evaluation of the rate constants of photophysical processes was carried out according to [26]. In this approach, the rate constant of singlet–singlet energy transfer is taken the same as the rate constant of internal conversion between the states localized on the donor and acceptor [18, 26].

RESULTS AND DISCUSSION

Figure 2 shows the compression isotherms of the mixed monolayers of polyampholyte and the studied dyes.

The isotherm of a fluorescein monolayer (curve *2*) is characteristic for the liquid phase [12]. The maximum area occupied by one dye molecule, which is equal to 0.5 ± 0.02 nm^2, was determined by extrapolation of the isotherm to zero pressure. The collapse pressure for the fluorescein monolayer is equal to 25 mN/m. Addition of polymer molecules reduces the specific molecular area, whereas the pressure of collapse is increased to 38 mN/m. In this case, the specific molecular area is equal to 0.42 ± 0.02 nm^2.

Molecules of oxazine-41 does not form a stable monolayer (curve *3*). Extrapolation of π to the zero value shows that the average area per dye molecule at a pressure of 10 mN/m is equal to 1.1 ± 0.02 nm^2. The isotherm of monolayer compression changes upon addition of polyampholyte. As can be seen from the figure, the monolayer is in the liquid phase with a specific molecular area of 0.54 ± 0.02 nm^2. The film is collapsed at 39 mN/m.

Overall, as can be seen from the isotherms, the addition of PDAOM to the dye films shifts the isotherms toward the smaller specific areas, which indicates a denser packing of the molecules of the luminophore and PDAOM.

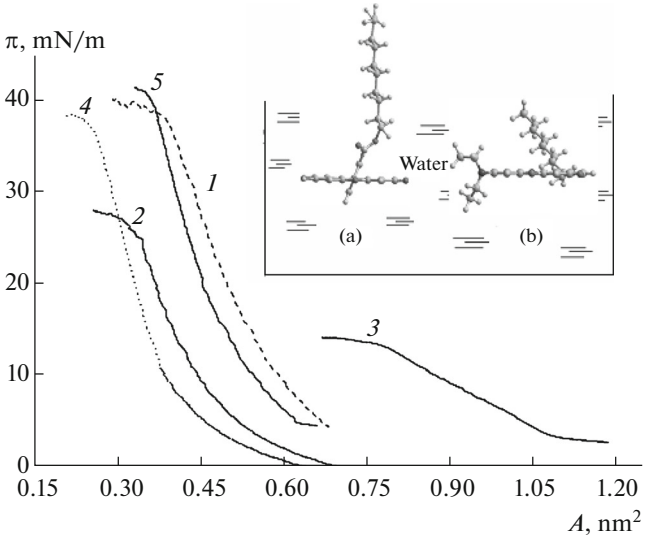

Fig. 2. Compression isotherms of mixed monolayers of (*1*) amphiphilic polyampholyte, (*2*) DEF, and (*3*) oxazine-41, and mixed monolayers (*4*) DEF-PDAOM, 20 mol %, and (*5*) oxazine-41-PDAOM, 10 mol %. Inset shows a schematic representation of the orientation of (a) DEF and (b) oxazine-41 (b) molecules on the water surface.

Computer simulation of the spatial conformation of DEF showed that, for the orientation of the xanthine fragment of the dye parallel to the water surface, specific area A is equal to 0.48 ± 0.02 nm^2. In this case, the benzoic fragment of the molecule is positioned at an angle of ≈70° to the plane of the water surface. The calculated value of the specific molecular area for oxazine is in good agreement with the experimental data for the mixed monolayer and with the value of 0.58 ± 0.02 nm^2 reported in [27, 28]. It can be concluded on the basis of the obtained data that, for a significant fraction of oxazine-41 molecules, the plane of the central nucleus is oriented parallel to the plane of the water surface. The spatial conformation of the molecules was calculated in vacuo by the method of molecular mechanics MM+ on the basis of the geometrical size of the molecules.

Next, we studied the interlayer energy transfer in LB films based on DEF and oxazine-41. Absorption and fluorescence spectra of the donor and acceptor are shown in Fig. 3a.

As can be seen, the absorption spectrum of the acceptor and the fluorescence spectrum of the donor have a significant degree of overlap, which is a prerequisite for singlet–singlet energy transfer. The location of the maxima of the donor and acceptor fluorescences allows their separate identification.

Figure 3b and Table 1 present data on the intensity and lifetimes of the fluorescence of the films of donor–acceptor pairs at various concentrations of the acceptor molecules. Photoexcitation of the samples was carried out within the absorption band of the energy donor. As is seen from Table 1, the acceptor molecules quench fluorescence of the energy donor. The increase in the concentration of oxazine in the LB films to 20 mol % results in almost complete quenching of the donor fluorescence. However, this is accompanied by the appearance of a fluorescence with the maximum at about 650 nm that matches the fluorescence band of the acceptor. Upon laser excitation of the acceptor films at $\lambda_{las} = 488$ nm, no fluorescence was recorded. Therefore, the long-wavelength fluorescence should be attributed to sensibilized fluorescence of the acceptor molecules resulting from the energy transfer from the donor molecules excited to a singlet state to the acceptor molecules in the ground state. As seen from Table 1, the intensity of the acceptor fluorescence in the LB films decreases with increasing the dye concentration. The observed quenching of the

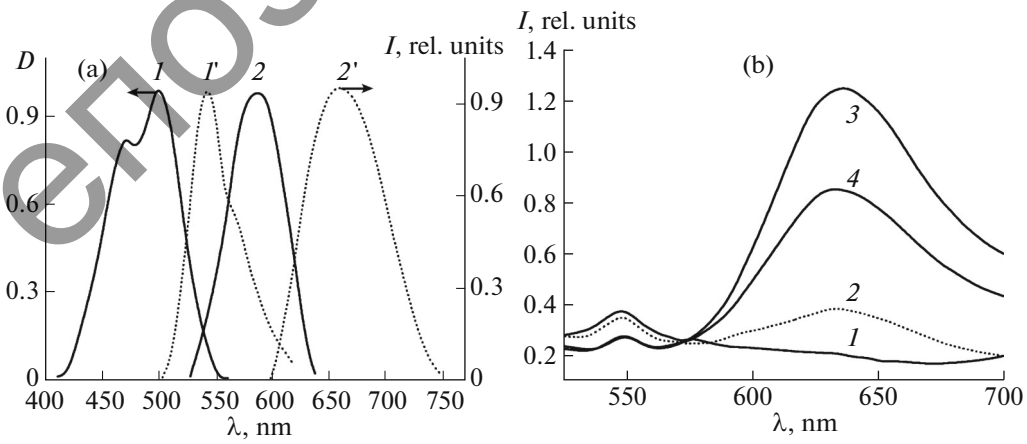

Fig. 3. (a) Normalized absorption (*1, 2*) and fluorescence (*1', 2'*) spectra of LB films of the energy donor (*1, 1'*) and the energy acceptor (*2, 2'*). (b) Fluorescence spectra ($\lambda_{exc} = 480$ nm) of the donor and acceptor LB films at various acceptor concentrations: (*1*) 0, (*2*) 5, (*3*) 10, and (*4*) 20 mol %.

Table 1. Lifetimes and intensities of donor and acceptor fluorescence (recorded at λ_{rec} = 542 and 655 nm, respectively) upon excitation within the absorption band of the donor

Acceptor concentration, mol %	I_D, rel. units	I_A, rel. units	E_{ET}	τ_{fl}, ns	
				τ_D	τ_A
0	0.38	0.2	–	0.48	–
5	0.35	0.38	0.11	0.425	1.3
10	0.27	1.25	0.27	0.35	0.96
20	0.27	0.86	0.54	0.22	0.85

acceptor fluorescence in the LB films is due to the aggregation of dye molecules in the film [28].

Kinetic measurements of the fluorescence decay of the donor in the absence and presence of the acceptor molecules also confirm the existence of the energy-transfer process between the LB layers of fluorescein and oxazine dye (Fig. 4a).

The measured fluorescence lifetimes (τ_{fl}) of the donor and sensibilizied fluorescence of the acceptor, as well as the efficiency of the energy transfer (E_{ET}), are presented in Table 1.

The value of E_{ET} was estimated from the expression [4]

$$E_{ET} = 1 - \frac{\tau_D}{\tau_{0D}}. \quad (1)$$

To study the dependence of the energy-transfer efficiency on the distance between DEF and oxazine-41, we prepared films in which the distance between the donor and acceptor layers ranged from 2.1 to 12.6 nm. Monolayers of palmitic acid with a known length of the molecules (~2 ± 0.2 nm) were used as the separating layer. Direct contact between the donor and acceptor through holes in the separating layer is negligible, because the holes occupy only a tiny part of the surface [20]. The donor and acceptor concentrations were constant and controlled by the optical density of the LB films. The contents of DEF and oxazine-41 in mixed LB films relative to PDAOM were 20 and 10 mol %, respectively.

Figure 4b shows the dependence of the fluorescence intensity of the donor on the distance between the donor and acceptor layers. As can be seen, the case of direct contact between the donor and acceptor layers is characterized by the most efficient quenching of the donor fluorescence. As the number of palmitic-acid monolayers between the donor and acceptor increases, the efficiency of the energy transfer decreases. The obtained data allowed us to estimate the critical radius of the energy transfer, R_0, defined as the distance between the donor and acceptor at which the transfer probability is equal to the probability of donor internal deactivation [4]. The obtained value of the critical radius, $R_0 = 3.5 \pm 0.2$ nm, is in good agreement with the values characteristic for energy transfer by the inductive-resonance mechanism [4].

It is known that the energy-transfer rate depends on the mutual orientation of the donor and acceptor molecules, which is characterized by an orientation factor in the Förster theory [4, 19]. To establish the mutual orientation, we performed quantum-chemical calculations for the energy-transfer process in the considered pair. The modeling was performed for nonamphiphilic analogues of DEF and oxazine-41, because preliminary calculations have shown that the methyl group of the hydrophobic fragments of the dye molecules does not participate in the formation of the electronically excited states. Experimental studies also confirm that the spectral behavior of the nonamphiphilic dye molecules is similar to their hydrophobic modifications [29, 30].

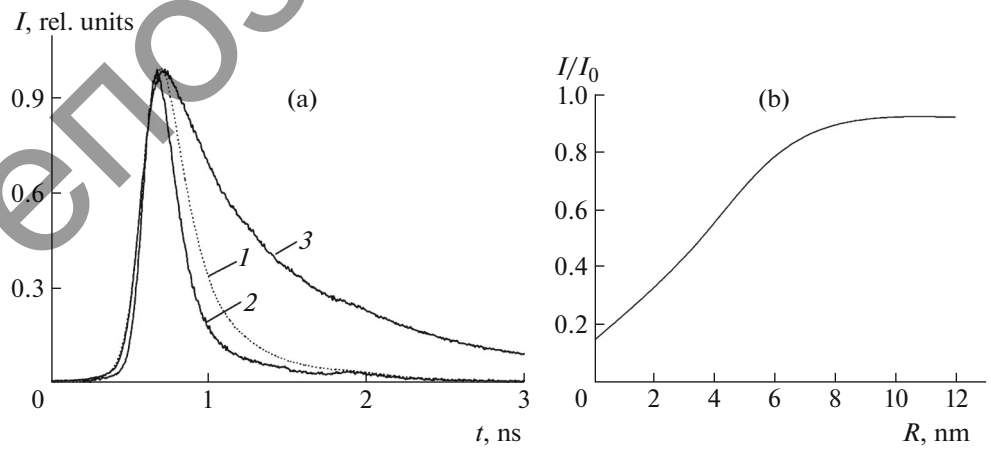

Fig. 4. (*1*) Decay kinetics of LB films of the donor, (*2*) donor in the presence of the acceptor (recorded at λ_{rec} = 542 nm), and (*3*) acceptor (recorded at λ_{rec} = 655 nm). (b) Dependence of the donor fluorescence intensity on the distance between the donor and acceptor layers.

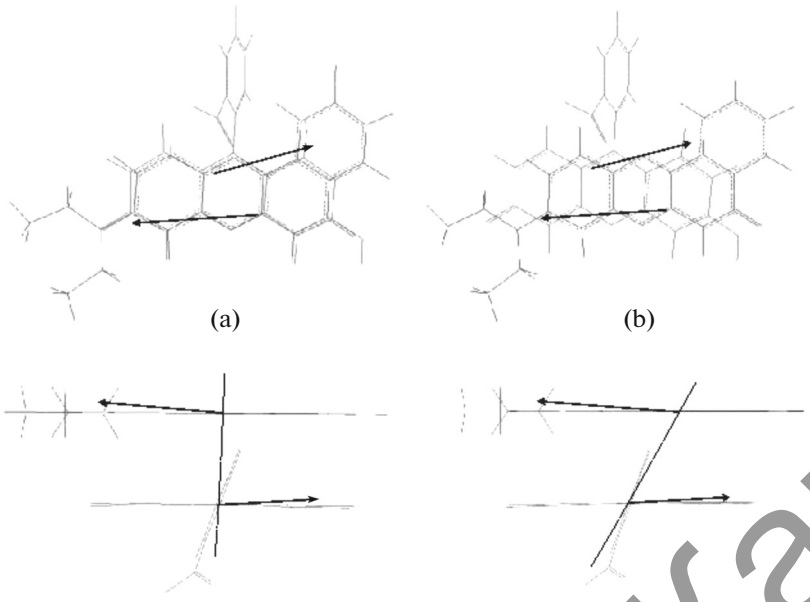

Fig. 5. Images of modeled conformations (a) I and (b) II of the donor–acceptor complex.

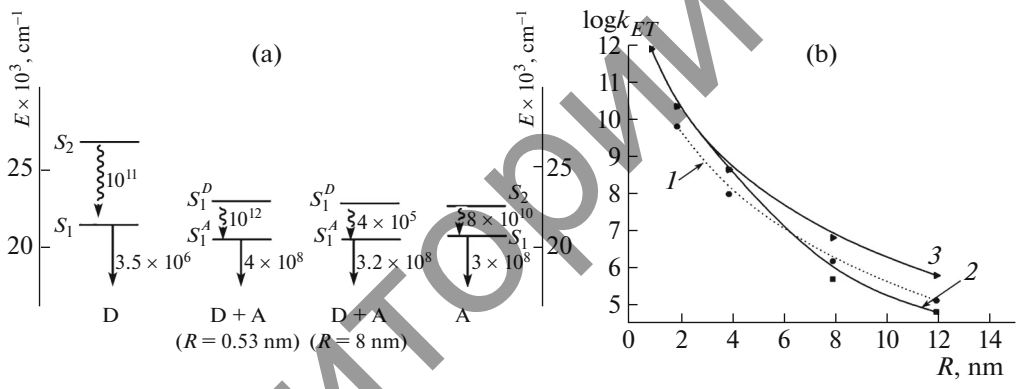

Fig. 6. (a) Scheme of electronic states and photophysical processes (rate constants in units s^{-1}) in the donor (D), acceptor (A) molecules, and in the donor–acceptor system D + A (in an arbitrary energy scale) depending on the distance between the molecules. (b) Dependence of k_{ET} on the distance between the donor and acceptor molecules: (*1*) experiment, (*2*) modeling for conformation I, and (*3*) modeling for conformation II.

On the basis of the obtained data on the compression isotherms for the dye monolayers and the data on the orientation of molecules on the phase interface, two conformations of the "sandwich" type (Fig. 5) were selected for further studies. The first conformation corresponds to the location of the donor and acceptor molecules strictly above each other in parallel planes. In the second conformation (conformation II), acceptor molecules are shifted along the long axis of the donor molecules (Fig. 5). The donor–acceptor distance was varied from 0.53 to 12 nm. The minimum distance was selected in such a way as to prevent overlapping of van der Waals radii of the molecules. The arrows in Fig. 6 shows the directions of the transition dipole moments in the studied molecules.

Consider the formation of electron-excited states of individual molecules. Table 2 shows the calculated results on the energy (E) of S_1, oscillator strength (f), and the nature of the S_0–S_i transitions in the fluorescein and oxazine molecules, as well as the quantum yield of fluorescence (φ), and the radiative-decay rate constant.

The calculation results reasonably well correlate with literature and experimental data [27, 29, 30].

The discrepancy in the calculated and experimental energies of electronically excited states of the acceptor with the experimental data is due to the fact that Nile red has solvatochromism properties and is highly affected by the solvent [28, 31]. Therefore, the calculated data are to be compared with the gas phase

Table 2. Results of calculation of spectral characteristics of donor and acceptor molecules

State	E, cm^{-1}	λ, nm	f	k_r, s^{-1}	λ_{exp}, nm	φ_{calc}
S_1, donor	21700	460	0.37	1.2×10^8	480	0.97
S_1, acceptor	21364	470	0.99	3.2×10^8	550	0.01

results for this molecule. In addition, the calculated quantum yield of the Nile red fluorescence in vacuum is about 0.01. This is consistent with the results of [31]. The reason for this is a fast interconversion from state S_1 to triplet states that are close in energy. In solutions, however, intermolecular interactions of oxazine with solvent molecules increase the energy of nearby triplet states, which prohibits interconversion transition to these states. Emission becomes the main decay channel of the S_1 state, so the fluorescence quantum yield increases.

Figure 6 shows the diagrams of the excited singlet states in the donor–acceptor complex and the rate constants of photophysical processes leading to their deactivation.

As seen from the figure, the energy transfer from the first excited state of the donor to the singlet state, which is localized mainly in the acceptor part of this complex, occurs during $t = 10^{-12}$ s.

Figure 6b shows calculated results for the dependence of the energy-transfer rate constant k_{ET} on the distance between the donor and acceptor molecules.

The values of k_{ET} for curve *1* were calculated according to the Förster–Dexter formula [4]

$$k_{ET} = \frac{1}{\tau_{0D}}\left(\frac{R_0}{R}\right)^6. \quad (2)$$

The dependence of the energy-transfer rate is a monotonically decreasing curve. As can be seen from the presented data, the efficiency of the energy transfer is low when the distance exceeds 8 nm, with the curves that represent the dependence of the energy-transfer rate on the donor–acceptor distance being different for different conformations. These differences can be explained as follows. The value of the orientation factor in the theory of the energy transfer is determined by the following parameters [4]:

$$\varphi^2 = (\cos\upsilon_{DA} - 3\cos\upsilon_{Dr}\cos\upsilon_{Ar})^2, \quad (3)$$

where υ_{DA} is the angle between the directions of the transition dipole moments in the donor and the acceptor and υ_{Dr} (υ_{Ar}) is the angle between the direction of the transition dipole moment in the donor (acceptor) molecule and the vector connecting the centers of gravity of the donor and acceptor molecules.

Since the orientation of the molecules in the film is conserved when a monolayer is transferred on the surface of solid substrates [28, 32], the angles of the transition dipole moments in the interacting molecules in the studied layers are not changed. However, it is not possible to predict how molecules will be located relative to each other in different planes. This means that angles υ_{Dr} and υ_{Ar} can be changed. As can be seen from Fig. 6b, calculated curve *2* does not coincide with curve *1* obtained from experimental data. This suggests that, in a multilayer film, the most likely orientation of the molecules is such that angles υ_{Dr} and υ_{Ar} will have smaller values. Estimates of the angles showed that the first angle changes from 83° to 64° in conformations I and II, respectively. Angle υ_{Ar} also decreases from 95° to 50°.

In order to further confirm the data obtained by the molecular mechanics method, we estimated the energy of the donor–acceptor complex in different conformations. The calculations showed that, in conformation I, the energy equals 62.6 kcal/mol, while in conformation II it is 51.2 kcal/mol. These results indicate a significant gain in energy for complex II. In addition, estimation of charges on the atoms of the luminophore molecules showed that the oxygen atom of the pironine fragment of the donor has a negative charge close to the charge of the oxygen atom of the pyridine ring in the acceptor molecule. For conformation I, this leads to mutual repulsion of these atoms from each other.

Thus, it can be argued that the donor and acceptor molecules located in different layers of the LB film are oriented parallel to each other, but shifted along the longer axis of the active chromophore.

CONCLUSIONS

Transfer of excitation energy between singlet electronic states of organic dyes molecules in the LB films was studied theoretically and experimentally. It is shown that the energy transfer is efficient at donor–acceptor distances of less than 4 nm. To predict the mutual orientation of the donor and acceptor molecules in different layers of LB films, we carried out calculations of the energy-transfer rate constant. The comparison of the calculated and experimental dependence of $k_{ET}(R)$ showed that the best correlation is observed in the case when the interacting particles are shifted relative to each other by about 0.12 nm in parallel planes.

The presented approach can be used to estimate the relative orientation of interacting particles in multimolecular ensembles.

REFERENCES

1. R. K. Clayton, *Photosynthesis: Physical Mechanisms and Chemical Patterns* (Cambridge Univ. Press, Cambridge, 1980).

2. J. R. Lakowicz, *Principles of Fluorescence Spectroscopy* (Kluwer/Plenum, New York, 2006).
3. S. K. Gorbatsevich, *Spectroscopy of Intermolecular Interactions. Nonlinear Effects* (Belorus. Gos. Univ., Minsk, 2002) [in Russian].
4. V. L. Ermolaev, E. N. Bodunov, E. V. Sveshnikova, and T. A. Shakhveredov, *Non-Radiative Electronic Excitation Energy Transfer* (Nauka, Leningrad, 1977) [in Russian].
5. N. Ibrayev, E. Seliverstova, A. Aimukhanov, and T. Serikov, Mol. Cryst. Liq. Cryst. **589**, 202 (2014). doi 10.1080/15421406.2013.872827
6. N. Ibrayev, E. Seliverstova, N. Nuraje, and A. Ishchenko, Mat. Sci. Semicond. Process., No. 31, 358 (2015). doi 10.1016/j.mssp.2014.12.006
7. E. B. Sveshnikova, L. Yu. Mironov, S. S. Dudar', and V. L. Ermolaev, Opt. Spectrosc. **113**, 607 (2012). doi 10.1134/S0030400X12120089
8. L. Yu. Mironov, E. B. Sveshnikova, and V. L. Ermolaev, Opt. Spectrosc. **119**, 77 (2015). doi 10.1134/S0030400X15070188
9. K. Kopra and H. Harma, New Biotechnol. **32**, 575 (2015). doi 10.1016/j.nbt.2015.02.007
10. D. Dey, Ja. Saha, A. Datta Roy, D. Bhattacharjee, S. Sinha, P. K. Paul, S. Chakraborty, and S. A. Hussain, Sens. Actuators B **204**, 746 (2014). doi 10.1016/j.snb.2014.08.029
11. N. Vusher, K. N. Drekhhage, M. Flesk, H. Kuhn, and D. Mobius, Mol. Cryst. Liq. Cryst. **2**, 199 (1967).
12. A. W. Adamson and A. P. Gast, *Physical Chemistry of Surfaces* (Wiley Interscience, New York, 1997).
13. D. Jankowski, P. Bojarski, P. Kwiek, and S. Rangełowa-Jankowska, Chem. Phys. **373**, 238 (2010). doi 10.1016/j.chemphys.2010.05.016
14. M. Gilbert and B. Albinsson, Chem. Soc. Rev. **44**, 845 (2015). doi 10.1039/C4CS00221K
15. E. N. Bodunov, M. N. Berberan-Santos, and J. M. G. Martinho, J. Luminesc. **96**, 269 (2002).
16. V. L. Ermolaev and E. B. Sveshnikova, Opt. Spectrosc. **119**, 642 (2015). doi 10.1134/S0030400X15100112
17. E. N. Bodunov and M. N. Berberan-Santos, Chem. Phys. **301**, 9 (2004). doi 10.1016/j.chemphys.2004.02.012
18. V. Ya. Artyukhov and G. V. Maier, Russ. J. Phys. Chem. A **75**, 1034 (2001).
19. V. L. Ermolaev, E. N. Bodunov, and E. B. Sveshnikova, Phys. Usp. **39**, 261 (1996).
20. N. Kh. Ibrayev and D. A. Afanasyev, Chem. Phys. Lett. **538**, 39 (2012). doi 10.1016/j.cplett.2012.04.024
21. O. V. Prezhdo, W. R. Duncan, and V. V. Prezhdo, Acc. Chem. Res. **41**, 339 (2008). doi 10.1021/ar700122b
22. H. Yan, H. Suyuan Zeng, and M. Niu, Appl. Surf. Sci. **349**, 163 (2015). doi 10.1016/j.apsusc.2015.04.211
23. C. B. Rafael, M. C. R. Melo, and K. Schultena, Biochim. Biophys. Acta **1850**, 872 (2015). doi 10.1016/j.bbagen.2014.10.019
24. S. A. Yeroshina, N. Kh. Ibrayev, S. E. Kudaibergenov, F. Rullens, M. Devillers, and A. Laschewsky, Thin Solid Films **516**, 2109 (2008). doi 10.1016/j.tsf.2007.05.056
25. V. Ya. Artyukhov and A. I. Galeva, Izv. Vyssh. Uchebn. Zaved., Fiz., No. 11, 96 (1986).
26. G. V. Maier, V. Ya. Artyukhov, and O. K. Bazyl', *Electronic-Excited States and Photochemistry of Organic Compounds* (Nauka, Novosibirsk, 1997) [in Russian].
27. V. I. Alekseeva, L. E. Marinina, L. P. Savvina, and N. Kh. Ibrayev, Mol. Cryst. Liq. Cryst. **427**, 159 (2005). doi 10.1080/15421400590892163
28. E. V. Seliverstova, N. Kh. Ibrayev, and S. E. Kudaibergenov, Russ. J. Phys. Chem. A **87**, 865 (2013). doi 10.1134/S003602441305021X
29. N. Kh. Ibrayev, V. I. Alekseeva, L. E. Marinina, and L. P. Savvina, Russ. J. Phys. Chem. A **82**, 860 (2008).
30. V. I. Alekseeva, N. Kh. Ibrayev, E. A. Luk'yanets, L. E. Marinina, L. P. Savvina, and D. Z. Satybaldina, Rus. J. Phys. Chem. **73**, 2004 (1999).
31. N. I. Selivanov, L. G. Samsonova, V. Ya. Artyukhov, T. N. Kopylova, Russ. Phys. J. **54**, 601 (2011). doi 10.1007/s11182-011-9658-4
32. N. Kh. Ibrayev, A. M. Zhunusbekov, and D. Z. Satybaldina, Opt. Spectrosc. **87**, 298 (1999).